Astron. Astrophys. 325, 511–515 (1997)

ASTRONOMY
AND
ASTROPHYSICS

High resolution radio imaging of the extremely distant quasars 1251–407, 1351–018, 1354–174 and 1508+572

S. Frey[1,2], **L.I. Gurvits**[2,3], **K.I. Kellermann**[4], **R.T. Schilizzi**[2,5], **and I.I.K. Pauliny-Toth**[6]

[1] FÖMI Satellite Geodetic Observatory, P.O. Box 546, H-1373 Budapest, Hungary
[2] Joint Institute for VLBI in Europe, P.O. Box 2, 7990 AA Dwingeloo, The Netherlands
[3] Astro Space Center of P.N. Lebedev Physical Institute, Leninsky pr. 53, Moscow 117924, Russia
[4] National Radio Astronomy Observatory, 520 Edgemont Road, Charlottesville, Virginia 22903-2475, USA
[5] Leiden Observatory, P.O. Box 9513, 2300 RA Leiden, The Netherlands
[6] Max-Planck-Institut für Radioastronomie, Auf dem Hügel 69, D-53121 Bonn, Germany

Received 28 May 1996 / Accepted 28 March 1997

Abstract. We present results of first epoch high resolution imaging observations of four extremely distant quasars. The sample includes the only two radio-loud quasars at redshift $z > 4$ known to the date of observations, 1251−407 (z = 4.46) and 1508+572 (z = 4.30). The 5 GHz observations of 1251−407, 1351−018 (z = 3.71) and 1354−174 (z = 3.15) were made with the VLBA in January 1995. The source 1508+572 was observed with the EVN in May 1995. The milliarcsecond scale structures of these quasars are dominated by compact cores. The two $z > 4$ quasars are unresolved on the baselines observed. We show that the apparently less prominent milliarcsecond scale extended radio structures in high redshift quasars than in their low redshift counterparts may be explained by the difference in spectral indices of the cores and jets.

Key words: galaxies: active – radio continuum: galaxies – galaxies: quasars: general

Table 1. Source parameters

Source	RA (2000)[a] (h)	(m)	(s)	Dec (2000)[a] (°)	(′)	(″)	S[b] (mJy)	z
1251−407	12	53	59.53	−40	59	30.7	220	4.46[c]
1351−018	13	54	06.90	−02	06	03.2	820	3.71[d]
1354−174	13	57	06.08[e]	−17	44	01.8[e]	970	3.15[d]
1508+572	15	10	02.92	+57	02	43.4	292[f]	4.30[g]

[a] IERS 1995
[b] total flux density at 5 GHz from Wright & Otrupcek 1990
[c] Shaver et al. 1996
[d] Véron-Cetty & Véron 1993
[e] Perley & Taylor 1996
[f] Gregory et al. 1996
[g] Hook et al. 1995

1. Introduction

Presently known quasars are found in the redshift range $0.01 < z < 5$. By studying quasars at different redshifts one can address two main questions: *(i)* whether their intrinsic properties show evidence of evolution with redshift characteristic for this class of objects and *(ii)* whether the observed properties of quasars at different redshifts have the imprint of a cosmological model.

Cosmological tests using compact radio source structures have already provided promising results. The apparent angular size-redshift relation for different samples of such sources shows clear non-Euclidean behaviour (Kellermann 1993, Gurvits 1994) suggesting the possibility of using this dependence to constrain the deceleration parameter (q_0) and the cosmological constant (Λ) (Krauss & Schramm 1993, Jackson & Dodgson 1996). The apparent proper motion-redshift dependence for superluminal sources may also place limits on q_0 (e.g. Vermeulen 1996). Proper motion measurements of two-sided VLBI jets observed at different redshifts may lead to the determination of q_0 and the Hubble constant (H_0) independently of any luminosity calibration (Pelletier & Roland 1989, Roland et al. 1993). Structural data on the highest redshift quasars are especially important for these studies since the differences in the models are greater at higher redshifts.

Here we present 5 GHz VLBI observations of four extremely high redshift quasars, including 1251−407 and 1508+572 which were the only radio-loud quasars at $z > 4$ known to the date of observations (Shaver et al. 1996, Hook et al. 1995). We also discuss whether there is any difference in the appearance of cores and jets between high and low redshift sources.

Send offprint requests to: S. Frey, 1st address

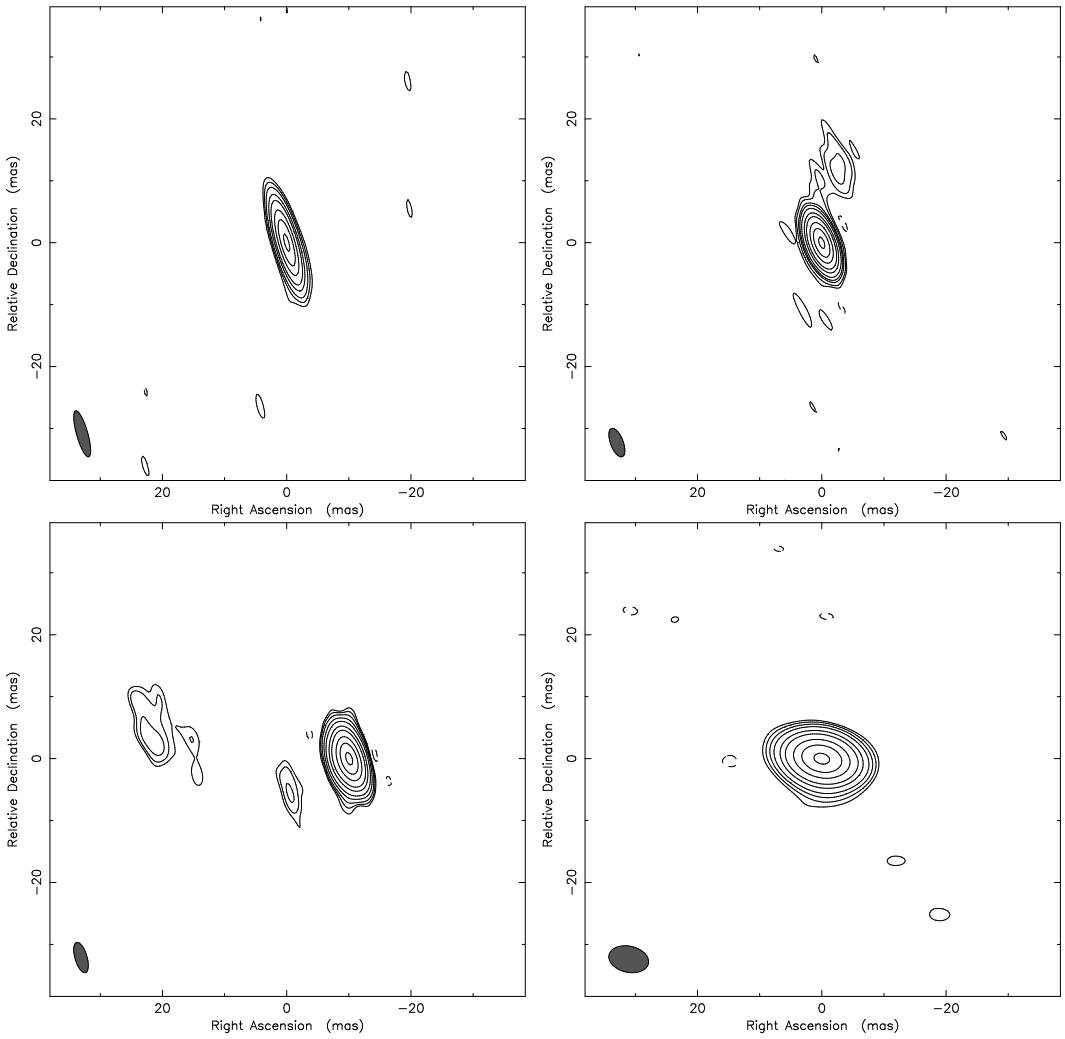

Fig. 1a–d. 5 GHz images of **a** 1251−407, **b** 1351−018, **c** 1354−174 and **d** 1508+572. Contour levels are: **a** –0.5, 0.5, 1, 2, 5, 10, 25, 50, 90% of the peak brightness of 162 mJy/beam; restoring beam is 7.7×1.8 mas at PA=16°; **b** –0.12, 0.12, 0.25, 0.6, 1, 2, 5, 10, 25, 50, 90% of the peak brightness of 886 mJy/beam; restoring beam is 4.9×2.0 mas at PA=21°; **c** –0.2, 0.2, 0.3, 0.5, 1, 2, 5, 10, 25, 50, 90% of the peak brightness of 807 mJy/beam; restoring beam is 5.1×1.9 mas at PA=16°; **d** –0.25, 0.25, 0.5, 1, 2, 5, 10, 25, 50, 90% of the peak brightness of 286 mJy/beam; restoring beam is 6.5×4.2 mas at PA=77°

2. Observations, calibration and data reduction

The source coordinates, redshifts and total flux densities are shown in Table 1. All observations were made at 5 GHz using left circular polarization.

The observations of 1251−407, 1351−018 and 1354−174 took place on 28 January 1995 using eight (for 1251−407) or nine (for 1351−018 and 1354−174) antennas of the NRAO Very Long Baseline Array (VLBA) with an effective bandwidth of 64 MHz. The data were correlated at the VLBA correlator in Socorro, NM, USA. The source 1508+572 was observed on 20 May 1995 using six western European antennas in the European VLBI Network (EVN). The data for 1508+572 were recorded with the Mk III VLBI system with an effective bandwith of 28 MHz. These data were correlated at the MPIfR correlator in Bonn, Germany. Parameters of the telescopes are summarized in Table 2.

Fringe-fitting and calibration were done using the NRAO AIPS package (Cotton 1995, Diamond 1995). The initial amplitude calibration was based on the system temperatures measured during the observations and the measured gain curves for each antenna. In the case of the VLBA observations, the amplitude calibration was adjusted by up to 2% using calibrator sources known to be unresolved or barely resolved with VLBA (1730–130 and 1127–145 on short baselines). The initial amplitude calibration for 1508+572 observed with EVN antennas had to be changed by up to 29% (in the case of Westerbork) based on observations of the calibrator source 1739+522 which is unresolved on the European baselines. Both the Caltech DIFMAP package (Shepherd et al. 1994) and NRAO AIPS package were used for self-calibration and imaging. The clean

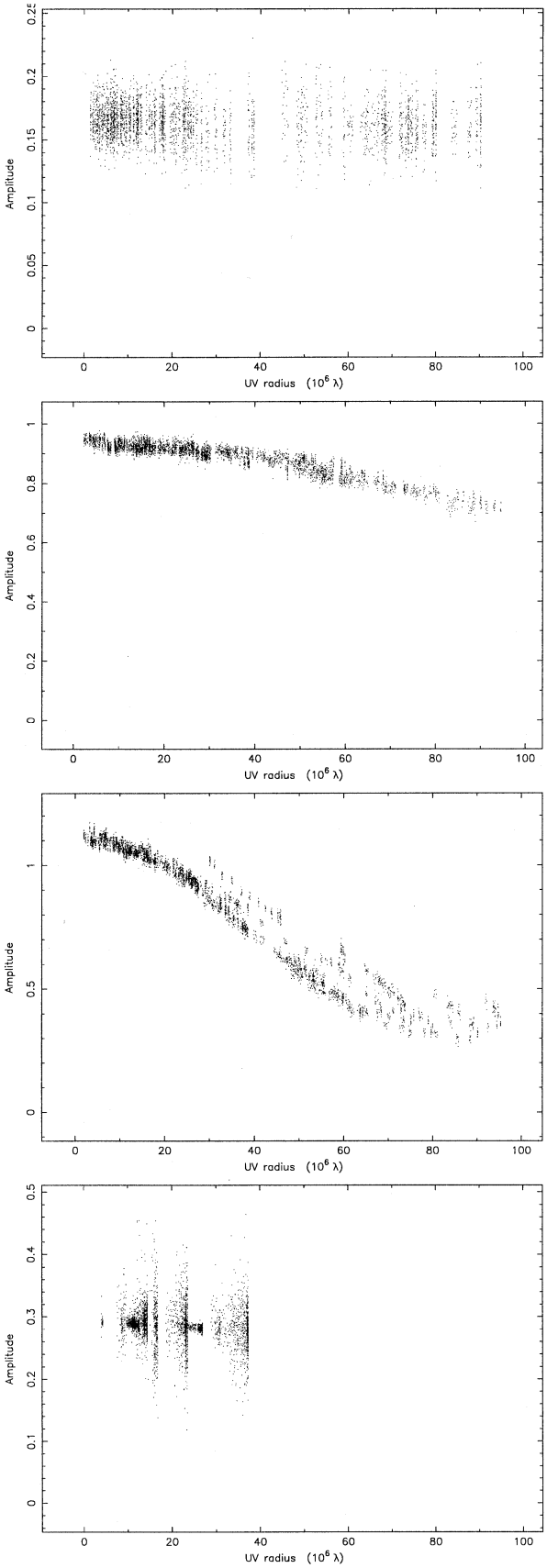

Fig. 2a–d. Correlated flux density (Jy) versus projected baseline length for **a** 1251−407, **b** 1351−018, **c** 1354−174 and **d** 1508+572

Table 2. VLBI telescopes and their characteristics at 5 GHz

Radio telescope	Diameter (m)	SEFD[a] (Jy)
VLBA[b]	25	300
Effelsberg	100	20
Jodrell Mk2	26	320
Medicina	32	296
Noto	32	187
Onsala	25	780
Westerbork	93[c]	108

[a] system equivalent flux density
[b] 8 or 9 identical antennas
[c] the telescope was used in phased array mode; an equivalent diameter is given.

maps shown in Fig. 1 are the results of the DIFMAP imaging process starting with point source models with flux densities consistent with the corresponding zero-spacing values. Table 3 summarizes the source model parameters obtained by model fitting using DIFMAP.

Plots of the correlated flux density values versus the projected baseline length are shown for each source in Fig. 2. Due to their unresolved nature, 1251−407 and 1508+572 appear to be reasonable amplitude calibrator and good phase-referencing sources at 5 GHz for the VLBA and EVN, respectively.

3. Comments on individual sources

3.1. 1251−407

This source is identified with a quasar at z = 4.46, the highest redshift radio-loud quasar found to the date of observations (Shaver et al. 1996). It remains practically unresolved on the VLBA baselines up to 90 Mλ (Fig. 2a).

3.2. 1351−018

The radio source 1351−018 has a redshift of z = 3.71. Earlier 20 cm VLA observation (Neff & Hutchings 1990) showed the source unresolved on ∼1.4 arcsecond scale. Our VLBA image (Fig. 1b) shows a dominant compact component and a very weak extension at a position angle of −13° with a peak brightness 20 times higher than the off-source rms noise. The angular separation of the peak of the extended emission from the core is 13 mas which corresponds to a linear distance of $l \simeq 90$ pc (H_0 = 80 km s^{-1} Mpc^{-1} and q_0 = 0.1 are assumed throughout the paper).

3.3. 1354−174

The source 1354−174 has the lowest redshift (z = 3.15) among the four sources discussed in this paper. Apart from the compact core, Fig. 1c shows two low brightness features in the eastern direction. Their peak brightness exceeds the image noise level by a factor of 20. The more distant, stronger component is separated

Table 3. Fitted elliptical Gaussian model parameters of the source structures

Source	Component	S (mJy)	r (mas)	Θ ($^\circ$)	a (mas)	b/a	Φ ($^\circ$)	Agreement factor
1251−407	A	164	–	–	0.8	0.2	25	0.66
1351−018	A	932	0	–	0.7	0.7	−24	1.06
	B	19	13.4	−13	7.5	0.0	72	
1354−174	A	1088	0	–	1.7	0.6	76	1.84
	B	16	10.5	131	22.0	0.0	−83	
	C	19	31.8	83	8.1	0.4	3	
1508+572	A	290	–	–	0.7	0.7	1	1.02

Notes to Table 3:
S flux density, r angular separation from the central component,
Θ position angle, a, b component major and minor axes,
Φ component major axis position angle,
agreement factor is the square root of reduced χ^2 (see e.g. Pearson 1995).
Position angles are measured from north through east.

from the core by 32 mas, corresponding to a linear separation of 200 pc.

3.4. 1508+572

This source has a redshift of z = 4.30. The source is unresolved on the relatively short intra-European baselines (up to 38 Mλ, Fig. 2d).

4. Discussion

In order to investigate parsec scale structural properties of radio-loud QSOs we study the sample of quasars imaged at 5 GHz in the Caltech-Jodrell (CJ) VLBI survey (Xu et al. 1995, Taylor et al. 1994, Henstock et al. 1995, Taylor et al. 1996) supplemented by the $z > 3$ quasars presented in this paper and Gurvits et al. (1992, 1994), and 1538+592 (Snellen 1996, private communication). The CJ survey contains sources over a broad range of redshifts ($0.2 < z < 3.9$). All $z > 3$ quasars imaged at 5 GHz with VLBI are included in our sample. For quasars with known redshifts (taken also from Véron-Cetty & Véron 1993, Vermeulen & Taylor 1995 and Vermeulen et al. 1996), we determined the flux density ratio of the brightest "jet" component and the core component. For this determination, we used the flux densities of the fitted model parameters given in the references. To compare regions of the same linear size in high and low redshift samples, we "fixed" the resolution at 7 pc, corresponding to ∼1 mas at $z \geq 1$ and to ∼1.5 mas at $z \simeq 0.5$. Only extended components outside this central region of 7 pc were considered in the following analysis. Similarly, if there were two or more components within the central region, the strongest one (presumably the core) was considered. In cases where no jet components were found according to the definition above, an upper limit to the jet flux density was determined based on the lowest contour level brightness and the beam size in the images. Some $z > 3$ sources imaged with considerably lower resolution than 1 mas were excluded from the analysis (0336−017, 1442+101 and 1508+572). The total number of quasars included was 151.

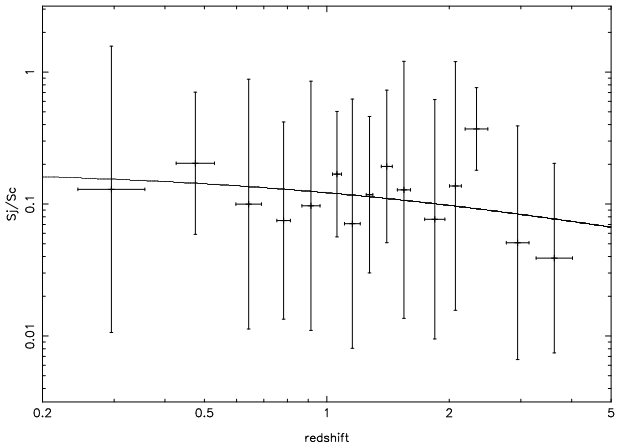

Fig. 3. S_j/S_c versus z for 151 quasars averaged over 15 bins. Error bars indicate the scatter of data within each bin. The solid curve indicates the best least squares fit calculated using unaveraged data

Compact radio cores are known to have flatter spectra than extended features associated with jets. Due to this difference, the ratio of apparent flux densities of a core and a jet observed at a fixed receiving frequency for two intrinsically identical objects but located at different redshifts will be different. Assuming that the radio spectrum of the components follows a power law with $S \propto \nu^\alpha$, the ratio of the jet and core flux densities is given by

$$S_j/S_c = k\nu_{em}^{\alpha_j-\alpha_c} \quad (1)$$

where α_j and α_c are the jet and core spectral indices and k is a constant, the emitted frequency ν_{em} is related to the observed frequency ν_{obs} by $\nu_{em} = \nu_{obs}(1 + z)$. S_j and S_c are defined as the flux densities of the strongest components outside and inside the 7 pc central region, respectively.

Fig. 3 shows values of S_j/S_c against z. For plotting purposes only, data are evenly averaged over 15 bins. Each bin

contains the same number of sources (10; in one case 11). Based on the simplest assumption that the intrinsic spectral properties of the sources are identical at different redshifts, one can estimate the spectral index difference $(\alpha_j - \alpha_c)$ which is consistent with the measured S_j/S_c values. The best least squares fit using all 151 points provides $\alpha_j - \alpha_c = -0.55 \pm 0.43$ as shown also in Fig. 3. The value obtained is consistent with what is known about core and jet spectra in well studied low redshift quasars. Quasars in general are known to have very compact flat spectrum self-absorbed cores with a radio spectral index $\alpha_c > -0.5$. The spectral indices of the extended radio features lie in the range $-1.3 < \alpha_j < -0.5$ (e.g. Kellermann & Owen 1988).

Although it can not be ruled out on the basis of this result, there is little reason to suppose that jet and core spectral indices for radio-loud quasars as a class of objects undergo significant change over large redshift range. Compact energetic radio sources observed with VLBI have relatively short radiative lifetimes (up to a few hundred years), which can be ignored on cosmological time scales even at the earliest cosmological epochs at which these objects are observable. Since the sources are subgalactic in size their radio structures are largely independent of the intergalactic medium (Kellermann 1993).

5. Conclusion

Investigating the weak trend we see in the apparent parsec scale radio morphology of quasars at different redshifts we suggest that the difference in their appearance at high and low redshifts at a fixed received frequency may naturally be explained by the difference in spectral indices of the cores and jets. In general, the steeper spectrum jets tend to be fainter with respect to the flat spectrum cores as the redshift, and therefore the rest-frame frequency, increases. The observed weak trend does not contradict the assumption of intrinsic similarity of quasar radio continuum spectral properties in the widest available range of redshifts. Together with other physical arguments (short radiative lifetime and small linear size), this conclusion supports the idea that radio-loud quasars are useful as "standard" objects for cosmological tests. New and more sensitive VLBI surveys of considerably larger samples of sources may provide data for a similar but statistically better established study.

Acknowledgements. We thank I. Snellen for providing data on 1538+592 prior to publication, H. Sanghera and A. Kemball for their advice on the data processing, and the referee for important suggestions. SF acknowledges financial support received from the Netherlands Organization for Scientific Research (NWO) and the Hungarian Space Office, and hospitality of JIVE and NFRA during his fellowship in Dwingeloo. LIG acknowledges partial support from the EU under contract no. CHGECT 920011, the NWO programme on the Early Universe and the European Commission, TMR Prgramme, Research Network Contract ERBFMRXCT 96–0034 "CERES". The National Radio Astronomy Observatory is operated by Associated Universities, Inc. under a Cooperative Agreement with the National Science Foundation.

References

Cotton W.D., 1995, in: Zensus J.A., Diamond P.J., Napier P.J. (eds.) Very Long Baseline Interferometry and the VLBA, ASP Conference Series 82, 189

Diamond P.J., 1995, in: Zensus J.A., Diamond P.J., Napier P.J. (eds.) Very Long Baseline Interferometry and the VLBA, ASP Conference Series 82, 227

Gregory P.C., Scott W.K., Douglas K., Condon J.J., 1996, ApJS 103, 427

Gurvits L.I., 1994, ApJ 425, 442

Gurvits L.I., Kardashev N.S., Popov M.V., Schilizzi R.T., Barthel P.D., Pauliny-Toth I.I.K., Kellermann K.I., 1992, A&A 260, 82

Gurvits L.I., Schilizzi R.T., Barthel P.D., Kardashev N.S., Kellermann K.I., Lobanov A.P., Pauliny-Toth I.I.K., Popov M.V., 1994, A&A 291, 737

Henstock D.R., Browne I.W.A., Wilkinson P.N., Taylor G.B., Vermeulen R.C., Pearson T.J., Readhead A.C.S., 1995, ApJS 100, 1

Hook I.M., McMahon R.G., Patnaik A.R., Browne I.W.A., Wilkinson P.N., Irwin M.J., Hazard C., 1995, MNRAS 273, L63

IERS, 1995, in: 1994 IERS Annual Report, Observatoire de Paris, Paris, II-28

Jackson J.C., Dodgson M., 1996, MNRAS 278, 603

Kellermann K.I., 1993, Nat 361, 134

Kellermann K.I., Owen F.N., 1988, in: Verschuur G.L., Kellermann K.I. (eds.) Galactic and Extragalactic Radio Astronomy (2nd ed.), Springer, Berlin, 563

Krauss L.M., Schramm D.N., 1993, ApJ 405, L43

Neff S.G., Hutchings J.B., 1990, AJ 100, 1441

Pearson T.J., 1995, in: Zensus J.A., Diamond P.J., Napier P.J. (eds.) Very Long Baseline Interferometry and the VLBA, ASP Conference Series 82, 267

Pelletier G., Roland J., 1989, A&A 224, 24

Perley R.A., Taylor G.B., 1996, The VLA Calibrator Manual, NRAO

Roland J., Charlot P., Lestrade J.-F., Miley G., Pelletier G., Schilizzi R., 1993, Class. Quantum Gravity 10, 251

Shaver P.A., Wall J.V., Kellermann K.I., 1996, MNRAS 278, L11

Shepherd M.C., Pearson T.J., Taylor G.B., 1994, BAAS 26, 987

Taylor G.B., Vermeulen R.C., Pearson T.J., Readhead A.C.S., Henstock D.R., Browne I.W.A., Wilkinson P.N., 1994, ApJS 95, 345

Taylor G.B., Vermeulen R.C., Readhead A.C.S., Pearson T.J., Henstock D.R., Wilkinson P.N., 1996, ApJS 107, 37

Vermeulen R.C., 1996, in: Ekers R., Fanti C., Padrielli L. (eds.) Extragalactic Radio Sources, Proc. IAU Symp. 175, Kluwer, Dordrecht (in press)

Vermeulen R.C., Taylor G.B., 1995, AJ 109, 1983

Vermeulen R.C., Taylor G.B., Readhead A.C.S., 1996, AJ 111, 1013

Véron-Cetty M.-P., Véron P., 1993, A Catalogue of Quasars and Active Nuclei (6th ed.), Scientific Report 13, ESO, Garching

Wright A.E., Otrupcek R.E. (eds.), 1990, PKSCAT90 - the Southern Radio Source Database, ATNF, Sydney

Xu W., Readhead A.C.S., Pearson T.J., Polatidis A.G., Wilkinson P.N., 1995, ApJS 99, 297

This article was processed by the author using Springer-Verlag LaTeX A&A style file *L-AA* version 3.